

# Mirror-Image Photoswitching of Individual Single-Walled Carbon Nanotube Transistors Coated with Titanium Dioxide \*\*

Song Liu, Jianming Li, Qian Shen, Yang Cao, Xuefeng Guo,\* Guoming Zhang, Chaoqun Feng, Jin Zhang, Zhongfan Liu, Michael L. Steigerwald, Dongsheng Xu,\* and Colin Nuckolls\*

The functionalization of nanoscale materials with stimuli-responsive components is an important tool for mimicking the functions of biological systems and conversion of external inputs to useful signals.<sup>[1–4]</sup> Recently, we reported the conductance switching of individual single-walled carbon nanotube transistors (SWNTTs) functionalized by photochromic molecules. The switching can be toggled back and forth between different conformations and is driven by external stimuli.<sup>[5,6]</sup> Herein, we report a combination of microfabrication and molecular self-assembly to produce functional devices formed from individual single-walled carbon nanotube field-effect transistors that are coated with photoactive TiO<sub>2</sub> quantum dots (Figure 1a). These studies utilize the inherent ultrasensitivity of SWNTTs that arises from their active surface being exposed to the environment, and is the basis for new types of sensors<sup>[1–3,5–8]</sup> and optoelectronic devices.<sup>[8–25]</sup> Importantly, the p-type semiconducting tubes show a large rapid conductance decrease upon exposure to UV light, the decrease reverses when the UV irradiation is switched off. In contrast, the mirror-image photoswitching effects are seen for ambipolar tubes when the negative and positive gate fields are applied.

Titanium dioxide has been extensively investigated owing to its widespread applications in photocatalysis and many other studies.<sup>[26,27]</sup> The feature of these quantum dots that we utilize here is that UV irradiation generates free electrons (e<sup>−</sup>) and holes (h<sup>+</sup>) as the active centers on the nanocrystal surface (Figure 1b).<sup>[26,27]</sup> We have investigated whether these carriers are able to fine-tune the electrical properties of individual SWNTTs. We synthesized highly crystalline, monodisperse anatase TiO<sub>2</sub> nanoparticles of 3–5 nm diameter (Figure S1 in the Supporting Information) that are derivatized with oleic acid,<sup>[28]</sup> because it has been demonstrated by us and other research groups<sup>[3,5]</sup> that the long alkane chain of oleic acid can noncovalently associate with the surface of carbon nanotubes and therefore act as an anchor to hold the photoactive TiO<sub>2</sub> nanoparticles close to the tube surface. As expected, on polydimethylsiloxane (PDMS) substrates, thin films of TiO<sub>2</sub> nanoparticles show reversible optical absorption changes in the range of 220–350 nm under UV irradiation (254 nm) and in the dark (Figure S2 in the Supporting Information). The absorption changes of these nanoparticles provide a basis for the reversible photoswitching effects described below.

SWNTTs were fabricated using a previously reported procedure.<sup>[5,6,20–24]</sup> Individual single-walled carbon nanotubes (SWNTs) of high electrical quality were grown by a chemical vapor deposition (CVD) process from CoMo-doped mesoporous SiO<sub>2</sub> catalyst particles using ethanol as the carbon source.<sup>[14,29,30]</sup> The catalyst particles were patterned on doped silicon wafers that had 300 nm of thermally grown SiO<sub>2</sub> on their surface. Au (50 nm) on Cr (5 nm) leads, which were separated by 20 μm, formed the source and drain contacts to an individual SWNT through thermal evaporation. Figure 1c shows a representative scanning electron micrograph (SEM) of an individual straight SWNT spanning source and drain electrodes on a silicon oxide surface. The highly doped silicon wafer served as a global back-gate electrode for the devices. These pristine devices were then directly functionalized by self-assembly of nanoparticles from solution. After immersion of the devices for around 10 minutes in a solution of TiO<sub>2</sub> nanoparticles in hexane (ca. 0.4 g L<sup>−1</sup>), they were removed from solution and rinsed with fresh hexane and acetone. Figure 1c also shows the high-resolution atomic force micrograph (AFM) of the same tube, which indicates the successful assembly of TiO<sub>2</sub> nanoparticles on the tube surface.

Figure 2a shows Raman spectra of another individual SWNT before and after assembly. The spectra were obtained using a micro-Raman spectroscope (Renishaw 1000) coupled with a confocal imaging microscope, with an excitation energy of 1.96 eV (632.8 nm) and a 1 μm excitation spot size. We

[\*] S. Liu, J. Li, Q. Shen, Y. Cao, Prof. X. Guo, G. Zhang, C. Feng, Prof. J. Zhang, Prof. Z. Liu, Prof. D. Xu  
Center for Nanochemistry  
Beijing National Laboratory for Molecular Sciences  
State Key Laboratory for Structural Chemistry of Unstable and Stable Species  
College of Chemistry and Molecular Engineering, Peking University  
Beijing 100871 (P. R. China)  
Fax: (+86) 10-6275-7789  
E-mail: guoxf@pku.edu.cn  
dsxu@pku.edu.cn

Dr. M. L. Steigerwald, Prof. C. Nuckolls  
Department of Chemistry and the  
Columbia University Center for Electronics of Molecular Nanostructures  
Columbia University, New York, NY 10027 (USA)  
E-mail: cn37@columbia.edu

[\*\*] We acknowledge primary financial support from FANEDD (no. 2007B21), MOST (2009CB623703), and NSFC (grant nos. 50873004, 50821061, and 20833001). This work was partly supported by NSFC (grant no. 50521201 and 20525309) and MOST (grant nos. 2006CB806102, 2007CB936201, and 2007CB936203). C.N. and M.L.S. acknowledge financial support from the Nanoscale Science and Engineering Initiative of the National Science Foundation under NSF Award Number CHE-0641523 and by the New York State Office of Science, Technology, and Academic Research (NYSTAR).

Supporting information for this article is available on the WWW under <http://dx.doi.org/10.1002/anie.200901018>.

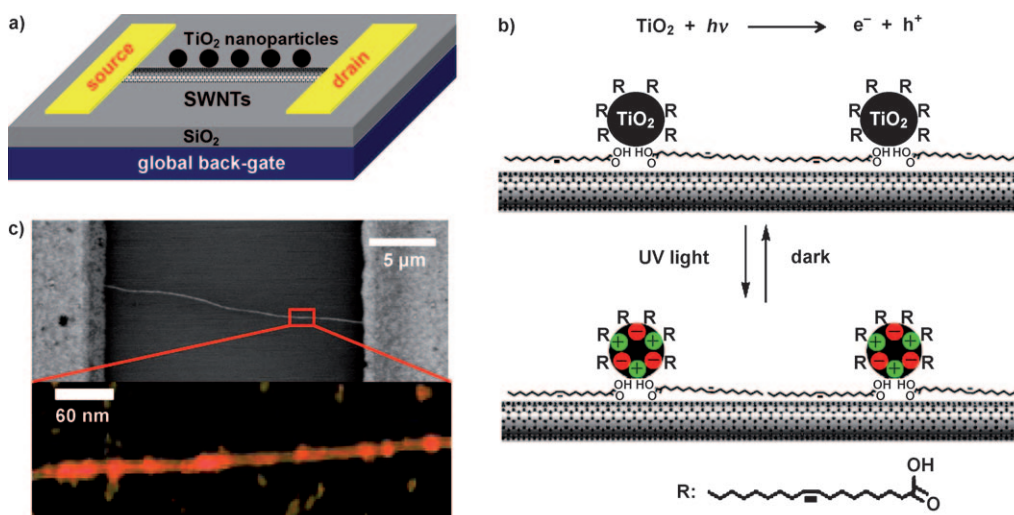


**Figure 1.** a) Representation of SWNTs coated by TiO<sub>2</sub> nanoparticles. b) Illustration of how TiO<sub>2</sub> nanoparticles effect the device characteristics under UV irradiation and in the dark. c) SEM and AFM images of a representative single tube on a silicon wafer assembled by TiO<sub>2</sub> nanoparticles. The tube is ca. 2.5 nm in diameter. The average diameter of TiO<sub>2</sub> nanoparticles is ca. 3.6 nm.

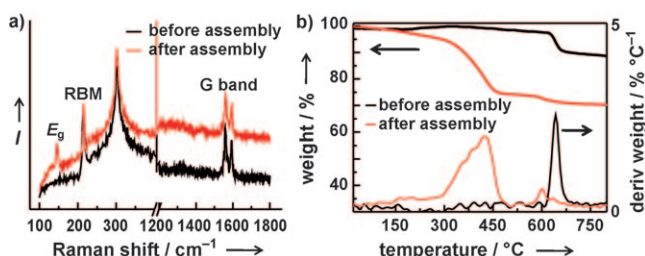


**Figure 2.** a) Raman spectra of an individual SWNT before (black) and after (red) assembly of oleic acid functionalized TiO<sub>2</sub> nanoparticles. b) TGA data of HiPco SWNT powders before (black) and after assembly (red) of oleic acid functionalized TiO<sub>2</sub> nanoparticles. The data were collected in nitrogen (10 °C min<sup>-1</sup>) from 20 to 900 °C.

observed a typical radial breathing mode (RBM) peak at approximately 215.3 cm<sup>-1</sup> before assembly, which corresponds to a SWNT with a diameter of approximately 1.15 nm.<sup>[31]</sup> Interestingly, after assembly, the Raman spectrum shows a new peak at approximately 144.3 cm<sup>-1</sup>, which is ascribed to the *E<sub>g</sub>* mode of highly crystalline anatase TiO<sub>2</sub> nanoparticles,<sup>[32]</sup> and the RBM and G-band peaks of the tube are essentially unchanged. To further confirm the successful attachment of TiO<sub>2</sub> nanoparticles on the tube surface, we carried out the studies of thermogravimetric analysis (TGA) in nitrogen (Figure 2b). The samples were prepared by mixing the commercial purified HiPco SWNT product (10 mg; Carbon Nanotechnologies Inc.) with the solution of oleic acid functionalized TiO<sub>2</sub> nanoparticles in hexane (ca. 0.4 g L<sup>-1</sup>, 50 mL). The precipitates were separated by centrifugation and rinsed with fresh hexane and acetone. As shown in Figure 2b, all the samples showed a considerable weight loss of approximately 20 wt % in the range from 300 °C to 460 °C, because of the decomposition of oleic acid, which suggests the presence of TiO<sub>2</sub> nanoparticles in these hybrid materials. High-resolution transmission electron microscope (TEM) experiments are consistent with the studies of Raman spectroscopy and TGA discussed above. We performed the

TEM experiments by using an individual CVD-grown SWNT suspended across a prefabricated slit on the SiO<sub>2</sub>/Si substrate.<sup>[33]</sup> The successful attachment of TiO<sub>2</sub> nanoparticles onto the tube surface is shown by a high-resolution TEM image (Figure S3 in the Supporting Information).

We found that the electrical characteristics of these transistors changed significantly after self-assembly. Figure 3a shows the source–drain current (*I<sub>D</sub>*) as a function of

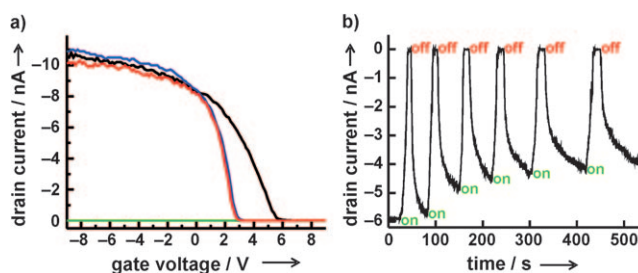


**Figure 3.** a) Changes in drain current of a p-type semiconducting device as a function of *V<sub>g</sub>* before assembly (black), after assembly (blue), under 254 nm UV irradiation for ca. 10 seconds (green), and after the UV light was switched off (red). Source–drain bias voltage –5 mV. b) Time course of the drain current of the same device while UV light was toggled on and off. Source–drain bias –5 mV. Gate bias –2 V.

the gate voltage (*V<sub>g</sub>*) at a fixed source–drain bias voltage (*V<sub>sd</sub>* = –5 mV) for a semiconducting tube in each step of the process. To eliminate possible artifacts from gate hysteresis, all of the current–voltage curves (*I*–*V*) were acquired on the same measurement cycle while scanning from positive to negative bias. We observed very stable *I*–*V* curves for a specific SWNT device in fixed experimental conditions, thus they can be used to detect photoswitching effects. Originally, this device indicates the typical p-type semiconducting FET behavior with the threshold voltage (*V<sub>th</sub>*) at approximately 5.7 V. Upon assembly of the materials, we observed that *V<sub>th</sub>* of

this device shifted to approximately 3.0 V, a change larger than 2.5 V, while the on-state resistance ( $R_{\text{on}}$ ) remains at a similar level. We also found that this shift in threshold voltage is universal for SWNTTs after the assembly. These results are consistent with those obtained from control experiments. We measured the device characteristics when devices were immersed in a solution of oleic acid in hexane (ca.  $1.5 \times 10^{-3} \text{ mol L}^{-1}$ ), removed, and rinsed with fresh hexane and acetone as described above for the nanoparticles. We observed shifts in  $V_{\text{th}}$  that were similar to those shown in Figure 3a (see Figure S4 in the Supporting Information for  $I$ - $V$  curves). Given the  $V_{\text{th}}$  shifts, we infer that a net negative charge is transferred from oleic acid to the nanotubes. These results imply that oleic acid molecules anchor to the surfaces of single-walled carbon nanotubes. As a result,  $\text{TiO}_2$  nanoparticles are adsorbed on the tube surfaces through oleic acid anchors (see the AFM picture in Figure 1c and the TEM image in Figure S3 in the Supporting Information).

Once  $\text{TiO}_2$  nanoparticles were tethered to the surface of the tubes, the device characteristics became very sensitive to UV light. We observed the reversible, fast, and significant changes in  $R_{\text{on}}$  when the devices were measured under UV irradiation and in the dark. Figure 3a shows such a photoswitching effect in a device when a handheld UV lamp (254 nm, a low intensity of ca.  $100 \mu\text{W cm}^{-2}$ ) was switched on and off. Upon UV irradiation at 254 nm, the initial high conductance state (blue curve in Figure 3a) became an insulating state (green curve). Moreover, the device nearly recovered its original high conductance state after the UV lamp was switched off (red curve). However, we notice that  $V_{\text{th}}$  did not change obviously after a whole photoswitching cycle, which implied that UV irradiation of  $\text{TiO}_2$  nanoparticles could generate charge traps that affect the carrier scattering rate while the carrier concentration and Schottky barrier at the nanotube-electrode junction essentially remain unchanged during the process (see Figure S5 in the Supporting Information for more data). Further experiments demonstrated that the photoswitching effect is a relatively fast process. Figure 3b shows the drain current as a function of time for the same device when a  $-5 \text{ mV}$  source-drain bias and  $-2 \text{ V}$  gate bias were applied. After only very brief UV irradiation, the drain current of the device decreased to its insulating state, that is, the device was essentially dead. Surprisingly, the switching process was reversible over several cycles when the UV light is toggled on and off. These photoswitching phenomena are quite reproducible as similar results are obtained in over 20 semiconducting devices (see Figure S5 in the Supporting Information).

Control experiments were performed to rule out potential artifacts. We examined the photoswitching effect of devices tethered only by oleic acid anchors, that is, devices treated with oleic acid but not with  $\text{TiO}_2$  quantum dots (see Figure S4b in the Supporting Information for the  $I$ - $V$  curves). Only a slight increase in drain current under UV irradiation was observed. The opposite phenomenon, that is, large current decreases, were reported to occur under UV irradiation in conventionally fabricated CVD-grown carbon nanotube devices without any photoactive species; these decreases mainly arise from the Schottky barrier modulation

caused by oxygen desorption.<sup>[34,35]</sup> In the present case, we used a much lower intensity of UV light (ca.  $100 \mu\text{W cm}^{-2}$ ). More importantly, the large quantity of oleic acid used on the nanotube surface in this study covers the metal-nanotube junctions, thus precluding the possibility of oxygen desorption under UV illumination. As a result, we believe that our oleic acid treated SWNTTs show such minimal current increase because of the intrinsic photoresponse of the tubes themselves under light irradiation.<sup>[36]</sup> In addition, a Schottky barrier formed at the junctions between the metal electrodes and the carbon nanotube could complicate the analysis during UV irradiation when the junctions are exposed to the photoactive nanoparticles.<sup>[5,11,37]</sup> To preclude this possibility, we have fabricated SWNTTs with these junctions covered by an insulating layer (polymethylmethacrylate, PMMA) that was patterned by using electron beam lithography. These junction-protected devices were then treated with a solution of  $\text{TiO}_2$  nanoparticles in hexane. We observed essentially the same photoswitching effect as that shown in Figure 3 and Figure S5 in the Supporting Information (an optical micrograph of the device and its electrical characteristics are given in Figure S6 in the Supporting Information). These results clearly prove that the photoactivity of  $\text{TiO}_2$  nanoparticles tethered on the surface of SWNTs is responsible for the changes in device characteristics, rather than a local change at the metal-nanotube junctions and subsequent Schottky barrier height modulation.

Based on the results mentioned above, we hypothesize that, during UV illumination, the free electrons generated by photoinduced charge separation migrate to the surface of quantum dots, thus producing scattering sites for the hole carriers that flow through the tubes. These active sites can scatter the hole carriers and therefore lower the mobility in the p-type semiconducting devices. Based on this hypothesis, it can be inferred that one should observe both the hole-current decrease and the electron-current increase in the same device when an ambipolar material is used. To prove this hypothesis, we decided to use ambipolar tubes, which show both electron and hole transport properties, in the same experiments.

By following the same sequential steps, we recorded the device characteristics of the ambipolar devices (a set of  $I$ - $V$  curves are shown in Figure S7 in the Supporting Information). After the assembly of  $\text{TiO}_2$  nanoparticles, the transition of these tubes from p-type to n-type shifted to more negative values. This result is consistent with those of control experiments (see Figure S8 in the Supporting Information), which indicate the successful attachment of  $\text{TiO}_2$  nanoparticles to the tube surfaces. Figure 4 shows the time traces of the drain current when the same device was held at different gate bias voltages. A fast, significant hole current decrease was observed when the gate bias was held at  $-9 \text{ V}$ , and the photoswitching process was reversible when the UV light was switched off (Figure 4a). However, when the gate bias was applied at  $2 \text{ V}$ , we observed, as expected, a fast large current increase under UV irradiation in the same device (Figure 4b). These results are reasonable because photoinduced free electrons of  $\text{TiO}_2$  nanoparticles can scatter the hole carriers in the p-type semiconductors and have an opposing function



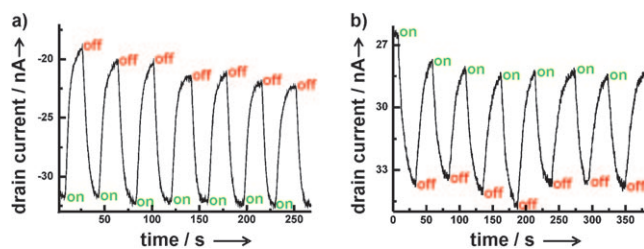


**Figure 4.** Time courses of the drain current of an ambipolar device after assembly while UV light was toggled on and off. a) Source–drain bias  $-5$  mV. Gate bias  $-9$  V. b) Source–drain bias  $5$  mV, gate bias  $2$  V.

as active sites to increase the electron current in the  $n$ -type materials. Moreover, all of the photoswitching processes show the significantly improved reversibility for at least 100 measurement cycles without obvious degradation, in comparison with the cases where the switching effects degraded quickly after a few measurement cycles.<sup>[5,17]</sup> In the control experiments, we observed slight, opposing changes in drain current when the negative gate bias was applied as described before and negligible changes when the positive gate bias was used (Figure S8 in the Supporting Information). These results strongly support the fact that the photoswitching effect of  $\text{TiO}_2$  nanoparticles is responsible for the reversible changes in device characteristics. It is remarkable that tuning the photoactivity of  $\text{TiO}_2$  realizes symmetric, opposing photoswitching effects, which are effectively mirror images, in the same device.

We have described a method to produce stimuli-responsive optoelectronic devices from individual SWNTTs functionalized by photoactive quantum dots. The  $p$ -type semiconducting tubes show fast significant current decrease under UV irradiation and excellent reversibility when the UV light is switched off. In contrast, the photoswitching effects of ambipolar tubes when different gate bias voltages are applied are the mirror-image of  $p$ -type semiconducting tubes. At a fundamental level, these results open up a novel route to designing new functioning devices that can accomplish a task similar to biological processes where external inputs can be converted into detectable signals. In addition, these results suggest that the presence of carbon nanotubes should facilitate photoinduced charge separation of  $\text{TiO}_2$  nanoparticles, which implies that these hybrid materials are good candidates for applications in sensing and photocatalysis.<sup>[38]</sup>

Received: February 22, 2009  
Published online: May 19, 2009

**Keywords:** field-effect transistors · nanostructures · nanotubes · photoswitching · titanium

- [1] M. Ouyang, J.-L. Huang, C. M. Lieber, *Acc. Chem. Res.* **2002**, *35*, 1018.
- [2] P. Avouris, *Acc. Chem. Res.* **2002**, *35*, 1026.
- [3] H. Dai, *Acc. Chem. Res.* **2002**, *35*, 1035.
- [4] S. W. Thomas, G. D. Joly, T. M. Swager, *Chem. Rev.* **2007**, *107*, 1339.
- [5] X. Guo, L. Huang, S. O'Brien, P. Kim, C. Nuckolls, *J. Am. Chem. Soc.* **2005**, *127*, 15045.

- [6] A. C. Whalley, M. L. Steigerwald, X. Guo, C. Nuckolls, *J. Am. Chem. Soc.* **2007**, *129*, 12590.
- [7] R. J. Chen, S. Bangsaruntip, K. A. Drouvalakis, N. W. S. Kam, M. Shim, Y. Li, W. Kim, P. J. Utz, H. Dai, *Proc. Natl. Acad. Sci. USA* **2003**, *100*, 4984.
- [8] D. S. Hecht, R. J. A. Ramirez, M. Briman, E. Artukovic, K. S. Chichak, J. F. Stoddart, G. Gruener, *Nano Lett.* **2006**, *6*, 2031.
- [9] E. Artukovic, M. Kaempgen, D. S. Hecht, S. Roth, G. Gruener, *Nano Lett.* **2005**, *5*, 757.
- [10] L. Hu, Y.-L. Zhao, K. Ryu, C. Zhou, J. F. Stoddart, G. Gruener, *Adv. Mater.* **2008**, *20*, 939.
- [11] T. Someya, P. Kim, C. Nuckolls, *Appl. Phys. Lett.* **2003**, *82*, 2338.
- [12] T. Someya, J. Small, P. Kim, C. Nuckolls, J. T. Yardley, *Nano Lett.* **2003**, *3*, 877.
- [13] Y.-L. Zhao, L. Hu, J. F. Stoddart, G. Gruener, *Adv. Mater.* **2008**, *20*, 1910.
- [14] L. Huang, Z. Jia, S. O'Brien, *J. Mater. Chem.* **2007**, *17*, 3863.
- [15] C. B. Winkelmann, I. Ionica, X. Chevalier, G. Royal, C. Bucher, V. Bouchiat, *Nano Lett.* **2007**, *7*, 1454.
- [16] R. A. Hatton, N. P. Blanchard, V. Stolojan, A. J. Miller, S. R. P. Silva, *Langmuir* **2007**, *23*, 6424.
- [17] J. M. Simmons, I. In, V. E. Campbell, T. J. Mark, F. Leonard, P. Gopalan, M. A. Eriksson, *Phys. Rev. Lett.* **2007**, *98*, 086802/1.
- [18] K. Maehashi, T. Katsura, K. Kerman, Y. Takamura, K. Matsumoto, E. Tamiya, *Anal. Chem.* **2007**, *79*, 782.
- [19] J. Borghetti, V. Derycke, S. Lenfant, P. Chenevier, A. Filoramo, M. Goffman, D. Vuillaume, J.-P. Bourgoign, *Adv. Mater.* **2006**, *18*, 2535.
- [20] A. K. Feldman, M. L. Steigerwald, X. Guo, C. Nuckolls, *Acc. Chem. Res.* **2008**, *41*, 1731.
- [21] X. Guo, A. A. Gorodetsky, J. Hone, J. K. Barton, C. Nuckolls, *Nat. Nanotechnol.* **2008**, *3*, 163.
- [22] X. Guo, M. Myers, S. Xiao, M. Lefenfeld, R. Steiner, G. S. Tulevski, J. Tang, J. Baumert, F. Leibfarth, J. T. Yardley, M. L. Steigerwald, P. Kim, C. Nuckolls, *Proc. Natl. Acad. Sci. USA* **2006**, *103*, 11452.
- [23] X. Guo, J. P. Small, J. E. Klare, Y. Wang, M. S. Purewal, I. W. Tam, B. H. Hong, R. Caldwell, L. Huang, S. O'Brien, J. Yan, R. Breslow, S. J. Wind, J. Hone, P. Kim, C. Nuckolls, *Science* **2006**, *311*, 356.
- [24] X. Guo, A. Whalley, J. E. Klare, L. Huang, S. O'Brien, M. Steigerwald, C. Nuckolls, *Nano Lett.* **2007**, *7*, 1119.
- [25] F. Wang, H. Gu, T. M. Swager, *J. Am. Chem. Soc.* **2008**, *130*, 5392.
- [26] M. R. Hoffmann, S. T. Martin, W. Choi, D. W. Bahnemann, *Chem. Rev.* **1995**, *95*, 69.
- [27] Y. Ohko, T. Tatsuma, T. Fujii, K. Naoi, C. Niwa, Y. Kubota, A. Fujishima, *Nat. Mater.* **2003**, *2*, 29.
- [28] Z. Zhang, X. Zhong, S. Liu, D. Li, M. Han, *Angew. Chem.* **2005**, *117*, 3532; *Angew. Chem. Int. Ed.* **2005**, *44*, 3466.
- [29] L. Huang, X. Cui, B. White, S. P. O'Brien, *J. Phys. Chem. B* **2004**, *108*, 16451.
- [30] L. Huang, S. J. Wind, S. P. O'Brien, *Nano Lett.* **2003**, *3*, 299.
- [31] Y. Yao, Q. Li, J. Zhang, R. Liu, L. Jiao, Y. T. Zhu, Z. Liu, *Nat. Mater.* **2007**, *6*, 293.
- [32] P. P. Lottici, D. Bersani, M. Braghini, A. Montenero, *J. Mater. Sci.* **1993**, *28*, 177.
- [33] K. Liu, W. Wang, Z. Xu, X. Bai, E. Wang, Y. Yao, J. Zhang, Z. Liu, *J. Am. Chem. Soc.* **2009**, *131*, 62.
- [34] R. J. Chen, N. R. Franklin, J. Kong, J. Cao, T. W. Tomblor, Y. Zhang, H. Dai, *Appl. Phys. Lett.* **2001**, *79*, 2258.
- [35] M. Shim, J. H. Back, T. Ozel, K.-W. Kwon, *Phys. Rev. B* **2005**, *71*, 205411.
- [36] M. Freitag, Y. Martin, J. A. Misewich, R. Martel, P. Avouris, *Nano Lett.* **2003**, *3*, 1067.
- [37] R. J. Chen, H. C. Choi, S. Bangsaruntip, E. Yenilmez, X. Tang, Q. Wang, Y.-L. Chang, H. Dai, *J. Am. Chem. Soc.* **2004**, *126*, 1563.
- [38] D. Eder, A. H. Windle, *Adv. Mater.* **2008**, *20*, 1787.